
AUTOMATING MODEL COMPARISON IN FACTOR GRAPHS

A PREPRINT

Bart van Erp^{1,*} Wouter W. L. Nuijten¹ Thijs van de Laar¹ Bert de Vries^{1,2}

¹Department of Electrical Engineering, Eindhoven University of Technology, Eindhoven, The Netherlands

²GN Hearing, Eindhoven, The Netherlands

June 12, 2023

ABSTRACT

Bayesian state and parameter estimation have been automated effectively in the literature, however, this has not yet been the case for model comparison, which therefore still requires error-prone and time-consuming manual derivations. As a result, model comparison is often overlooked and ignored, despite its importance. This paper efficiently automates Bayesian model averaging, selection, and combination by message passing on a Forney-style factor graph with a custom mixture node. Parameter and state inference, and model comparison can then be executed simultaneously using message passing with scale factors. This approach shortens the model design cycle and allows for the straightforward extension to hierarchical and temporal model priors to accommodate for modeling complicated time-varying processes.

Keywords Factor graphs · Message passing · Model averaging · Model combination · Model selection · Probabilistic inference · Scale factors

1 Introduction

The task of evaluating the performance of a model is a fundamental and very useful task in the field of machine learning. Model evidence is an excellent and principled performance measure, which can be used for comparing different models. Comparing different models given a set of observations is subject to prior beliefs about which models are preferred. The uncertainty arising from prior beliefs and limited observations can be naturally included through the use of Bayes' theorem

$$p(m | D) = \frac{p(D | m)p(m)}{p(D)}, \quad (1)$$

which describes the posterior probabilities $p(m | D)$ for a set of models m by comparing the different model evidences $p(D | m)$ and prior beliefs $p(m)$ and by normalizing with the marginal model evidence $p(D) = \sum_m p(D | m)p(m)$. Starting from Bayes' rule we can obtain different comparison methods such as Bayesian model averaging, selection, and combination [1], which we will formally introduce in Section 4. We will use Bayesian model comparison as an umbrella term for these three methods throughout this paper.

Despite the elegance of the Bayesian approach to model comparison, their application is often hindered in practice. Model comparison is often regarded as a separate task, whereas it submits to the same Bayesian formalism as state and parameter estimation. An important reason for skipping the model comparison stage in a modelling task is that the computation of model evidence $p(D | m)$ is in most cases not automated and therefore still requires error-prone and time-consuming manual derivations, in spite of its importance and the potential performance improvement that can be achieved by including a Bayesian model combination stage in the modeling process [1].

The connection between state and parameter inference, and model comparison has been explored recently by [2, 3]. They frame the problem of model comparison as an inference task on a mixture model, which is obtained by combining

*Correspondence: b.v.erp@tue.nl

the individual models with mixture weights representing the model selection variable. However, their exposition is based on relatively simple examples that do not easily generalize to more complex models for the model selection variable and for the individual cluster components. This lack of automatability hinders their approach from being successfully applied in practice. Alongside this approach, [4] has introduced the concept of ‘gates’, which allow for the generic specification of mixture models in which inference can be automated. Despite the universality of their approach, their inference procedure does not support exact inference but instead relies on variational inference [5–7] and expectation propagation [8]. As a result, their mixture selection variable is only updated based on local contributions to the model performance, disregarding the performance contributions of the rest of the models. Therefore their approach does not represent true Bayesian model comparison and can be very sensitive to the initialization of the inference algorithm, which has the potential to yield suboptimal inference results.

This paper is positioned between the mixture model and ‘gates’ approaches of [2] and [4], respectively. Specifically, we specify the mixture models of [2] as a factor graph with a custom mixture node for which we derive automatable message passing update rules, which performs both parameter and state estimation, and model comparison. These update rules generalize model comparison for arbitrary models, as the operations of the mixture node are ignorant about the adjacent subgraphs. Based on this generalization, we recover three common model comparison methods: model averaging, selection, and combination.

In short, this paper derives automated Bayesian model comparison using message passing in a factor graph. After reviewing factor graphs and message passing-based probabilistic inference in Section 2, we make the following contributions:

1. We show that Bayesian model comparison can be performed through message passing in a graph where the individual model performances are captured in a single factor node as described in Section 3.1.
2. We specify a universal mixture node and derive a set of custom message passing update rules in Section 3.2. Performing probabilistic inference with this node in conjunction with scale factors yields different Bayesian model comparison methods.
3. Bayesian model averaging, selection, and combination are recovered and consequently automated in Sections 4.1–4.3 by imposing a specific structure or local constraints on the model selection variable m .

We verify our presented approach in Section 5.1. We illustrate its use for models with both continuous and discrete random variables in Section 5.2.1, after which we continue with an example of voice activity detection in Section 5.2.2 where we add temporal structure on m . Section 6 discusses our approach and Section 7 concludes the paper.

2 Background material

This section aims to provide a concise review of factor graphs and message passing algorithms as we deem these concepts essential to appreciate our core contributions which we present in Sections 3 and 4. This review is intentionally not exhaustive, instead we provide references to works that help to obtain a deeper understanding about the material covered here. In Section 2.1 we introduce factor graphs as a way to visualize factorizable (probabilistic) models. Section 2.2 then describes how probabilistic inference can be efficiently performed through message passing utilizing the inherent factorization of the model. The model evidence can be tracked locally with message passing using scale factors as described in Section 2.3. Finally, Section 2.4 introduces the variational free energy as a bound on the model evidence.

2.1 Forney-style factor graphs

A factor graph is a specific type of probabilistic graphical model. Here we use the Forney-style factor graph (FFG) framework as introduced in [9] with notational conventions adopted from [10] to visualize our probabilistic models. An FFG can be used to represent a factorized function

$$f(s) = \prod_{a \in \mathcal{V}} f_a(s_a), \quad (2)$$

where s collects all variables in the function. The subset $s_a \subseteq s$ contains all argument variables of a single factor f_a . FFGs visualize the factorization of such a function as a graph $\mathcal{G} = (\mathcal{V}, \mathcal{E})$, where nodes \mathcal{V} and edges $\mathcal{E} \subseteq \mathcal{V} \times \mathcal{V}$ represent factors and variables, respectively. An edge connects to a node only if the variable associated with the edge is an argument of the factor associated with the node. Nodes are indexed by the variables a , b , and c , where edges are indexed by i and j unless stated otherwise. The set of edges connected to node $a \in \mathcal{V}$ is denoted by $\mathcal{E}(a)$ and the

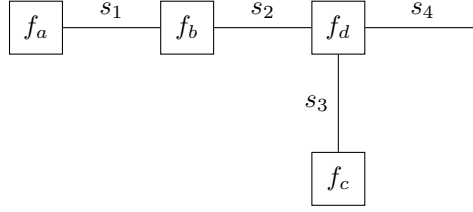


Figure 1: A Forney-style factor graph representation of the factorized function in (3).

set of nodes connected to edge $i \in \mathcal{E}$ is referred to as $\mathcal{V}(i)$. As an example consider the model $f(s_1, s_2, s_3, s_4)$ with factorization

$$f(s_1, s_2, s_3, s_4) = f_a(s_1)f_b(s_1, s_2)f_c(s_3)f_d(s_2, s_3, s_4) \quad (3)$$

The FFG representation of (3) is shown in Figure 1. For a more thorough review of factor graphs, we refer the interested reader to [10, 11].

2.2 Sum-product message passing

Consider the normalized probabilistic model

$$p(y, s) = \prod_{a \in \mathcal{V}} f_a(y_a, s_a), \quad (4)$$

with observed and latent sets of variables y and s , respectively. Note here that the subset $y_a \subseteq y$ can be empty, for example when dealing with prior distributions. Upon observing the realizations \hat{y} , the corresponding model $p(y = \hat{y}, s)$ becomes unnormalized. Probabilistic inference in this model then concerns the computation of the posterior distribution over the latent variables $p(s | y = \hat{y})$ and of the model evidence $p(y = \hat{y})$ as $p(y = \hat{y}, s) = p(s | y = \hat{y})p(y = \hat{y})$. Consider the global integration over all variables in (4) except for s_j as $\int p(y = \hat{y}, s) ds_{\setminus j}$ ¹. This large global integration can be performed through a set of smaller local computations as a result of the assumed factorization in (4). These smaller local computations can be considered to summarize the part of the graph that is being integrated over and are termed messages, which graphically can be interpreted to propagate over the edges in the graph. These messages are denoted by μ and can be locally computed on the graph. The sum-product message $\vec{\mu}_{s_j}(s_j)$ flowing out of the node $f_a(y_a = \hat{y}_a, s_a)$ with incoming messages $\vec{\mu}_{s_i}(s_i)$ is given by [12]

$$\vec{\mu}_{s_j}(s_j) = \int f_a(y_a = \hat{y}_a, s_a) \prod_{i \neq j} \vec{\mu}_{s_i}(s_i) ds_{a \setminus j}. \quad (5)$$

We represent edges in the graph by arbitrarily directed arrows in order to distinguish between forward and backward messages propagating in or against the direction of an edge s_j as $\vec{\mu}_{s_j}(s_j)$ and $\overleftarrow{\mu}_{s_j}(s_j)$, respectively. Following this approach, the global integration reduces to the product of the messages of the variable of interest as $\int p(y = \hat{y}, s) ds_{\setminus j} = \vec{\mu}_{s_j}(s_j)\overleftarrow{\mu}_{s_j}(s_j)$ for acyclic models.

Posterior distributions on edges and around nodes can then be computed according to

$$p(s_j | y = \hat{y}) = \frac{\vec{\mu}_{s_j}(s_j)\overleftarrow{\mu}_{s_j}(s_j)}{\int \vec{\mu}_{s_j}(s_j)\overleftarrow{\mu}_{s_j}(s_j) ds_j} \quad (6)$$

and

$$p(s_a | y = \hat{y}) = \frac{f_a(y_a = \hat{y}_a, s_a) \prod_{i \in \mathcal{E}(a)} \vec{\mu}_{s_i}(s_i)}{\int f_a(y_a = \hat{y}_a, s_a) \prod_{i \in \mathcal{E}(a)} \vec{\mu}_{s_i}(s_i) ds_a}, \quad (7)$$

respectively [13].

Derivations of the message passing update rule in (5) by phrasing inference as a constrained Bethe free energy minimization procedure are presented in [13]. Through a similar procedure one can obtain alternative message passing algorithms such as variational message passing [5–7], expectation propagation [8], expectation maximization [14] and hybrid algorithms.

¹Integrals are taken over the support over the variables. If a variable is discrete-valued, integral operators will be replaced with summation operators. For a consistent exposition of our work, we use integral operators throughout the paper.

2.3 Scale factors

The previously discussed integration $\int p(y = \hat{y}, s) ds_{\setminus j}$ can be represented differently as

$$\int p(y = \hat{y}, s) ds_{\setminus j} = p(y = \hat{y}) \int p(s | y = \hat{y}) ds_{\setminus j} = p(y = \hat{y})p(s_j | y = \hat{y}), \quad (8)$$

where $p(s_j | y = \hat{y})$ is the marginal distribution of s_j . The implications of this result are significant: the product of two colliding sum-product messages $\vec{\mu}_{s_j}(s_j)\vec{\mu}_{s_j}(s_j)$ in an acyclic graph results in the scaled marginal distribution $p(y = \hat{y})p(s_j | y = \hat{y})$. Because of the normalization property of $p(s_j | y = \hat{y})$ it is possible to obtain both the normalized posterior $p(s_j | y = \hat{y})$ as the model evidence $p(y = \hat{y})$ on any edge and around any node in the graph.

Theorem 2.1. *Consider an acyclic Forney-style factor graph $\mathcal{G} = (\mathcal{V}, \mathcal{E})$. The model evidence of the corresponding model $p(y = \hat{y}, s)$ can be computed at any edge in the graph as $\int \vec{\mu}_{s_j}(s_j)\vec{\mu}_{s_j}(s_j) ds_j$ for all $j \in \mathcal{E}$ and at any node in the graph as $\int f_a(y_a = \hat{y}_a, s_a) \prod_{i \in \mathcal{E}(a)} \vec{\mu}_{s_i}(s_i) ds_a$ for all $a \in \mathcal{V}$.*

Proof. See Appendix A.1. □

What enables this local computation of the model evidence is the scaling of the messages resulting from the equality in (5). As a result, the messages $\vec{\mu}_{s_j}(s_j)$ can be decomposed as

$$\vec{\mu}_{s_j}(s_j) = \vec{\beta}_{s_j} \vec{p}_{s_j}(s_j), \quad (9)$$

where $\vec{p}_{s_j}(s_j)$ denotes the probability distribution representing the normalized functional form of the message $\vec{\mu}_{s_j}(s_j)$. The term $\vec{\beta}_{s_j}$ denotes the scaling of the message $\vec{\mu}_{s_j}(s_j)$, also known as the scale factor [15, Ch.6], [16]. Scale factors can be interpreted as local summaries of the model evidence that are passed along the graph.

2.4 Variational free energy

In practice, however, the computation of the model evidence and therefore the posterior distribution is intractable. Variational inference provides a generalized view that supports probabilistic inference in these types of models by approximating the exact posterior $p(s | y = \hat{y})$ with a variational posterior $q(s)$ that is constrained to be within a family of distributions $q \in \mathcal{Q}$. Variational inference optimizes (the parameters of) the variational distribution $q(s)$ by minimizing the variational free energy (VFE) of a single model, defined as

$$F[q] = \mathbb{E}_{q(s)} \left[\ln \frac{q(s)}{p(y = \hat{y}, s)} \right] = \text{KL}[q(s) \parallel p(s | y = \hat{y})] - \ln p(y = \hat{y}), \quad (10)$$

through for example coordinate or stochastic gradient descent.

The variational free energy can serve as a bound to the model evidence in (1) for model comparison [17, Ch. 10.1.4], [18, 19]. It is important to emphasize that the VFE not only encompasses the model evidence but also the Kullback-Leibler (KL) divergence between the variational and exact posterior distributions obtained from the inference procedure.

3 Universal mixture modeling

This section derives a custom factor node that allows for performing model comparison as an automatable message passing procedure in Section 4. In Section 3.1 we specify a variational optimization objective for multiple models at once, where the optimization of the model selection variable can be rephrased as a probabilistic inference procedure on a separate graph with a factor node encapsulating the model-specific performance metrics. Section 3.2 further specifies this node and derives custom message passing update rules that allow for jointly computing (1) and for performing state and parameter inference.

Before continuing our discussion, let us first describe the notational conventions adopted throughout this section. In Section 2 only a single model was considered. Here we will cover K normalized models, selected by the model selection variable m , which comprises a 1-of- K binary vector with elements $m_k \in \{0, 1\}$ constrained by $\sum_{k=1}^K m_k = 1$. The individual models $p(y_k, s_k | m_k = 1)$ are indexed by k , where y_k and s_k collect the observed and latent variables in that model.

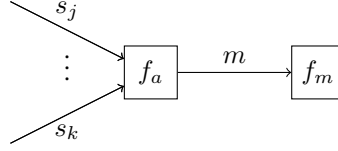


Figure 2: Subgraph containing the model selection variable m . The node f_m terminates the subgraph and is defined in (14).

3.1 A variational free energy decomposition for mixture models.

Consider the normalized joint model

$$p(y, s, m) = p(m) \prod_{k=1}^K p(y_k, s_k | m_k = 1)^{m_k} \quad (11)$$

specifying a mixture model over the individual models $p(y_k, s_k | m_k = 1)$, with a prior $p(m)$ on the model selection variable m and where $y = \bigcup_{k=1}^K y_k$ and $s = \bigcup_{k=1}^K s_k$. Based on this joint model let us define its variational free energy F as

$$\begin{aligned} F[q] &= \mathbb{E}_{q(s, m)} \left[\ln \frac{q(s, m)}{p(y = \hat{y}, s, m)} \right], \\ &= \mathbb{E}_{q(m)} \left[\ln \frac{q(m)}{p(m)} \right] + \mathbb{E}_{q(m)} \left[\prod_{k=1}^K (F_k[q])^{m_k} \right], \end{aligned} \quad (12)$$

in which the joint variational posterior $q(s, m)$ factorizes as $q(s, m) = q(m) \prod_{k=1}^K q(s_k | m_k = 1)^{m_k}$ and where F_k denotes the variational free energy of the k^{th} model. Derivations are provided in Appendix B.1.

This definition has also appeared in a similar form in [17, Ch.10.1.4] and in the reinforcement learning and active inference community as an approach to policy selection [20, Sec.2.1]. From this definition, it can be noted that the VFE for mixture models can also be written as

$$F[q] = \mathbb{E}_{q(m)} \left[\ln \frac{q(m)}{p(m) f_m(m)} \right] \quad (13)$$

where

$$f_m(m) = \prod_{k=1}^K \exp(-F_k[q])^{m_k}. \quad (14)$$

This observation implies that the obtained VFEs of the individual submodels can be combined into a single factor node f_m , representing a scaled categorical distribution, which terminates the edge corresponding to m , as shown in Figure 2. The specification of f_m allows for performing inference in the overcoupling model following existing inference procedures, similarly as in the individual submodels. This follows in line with the validity of Bayes' theorem in (1) for both state and parameter inference, and model comparison. Importantly, the computation of the VFE in acyclic models can be automated [13]. Therefore, model comparison itself can also be automated. For cyclic models, one can resort to approximating the VFE with the Bethe free energy [13, 21].

In practice the prior model $p(m)$ might have hierarchical or temporal dynamics, including additional latent variables. These can be incorporated without loss of generality due to the factorizable structure of the joint model, supported by the modularity of factor graphs and the corresponding message passing algorithms, as shown in Figure 2

3.2 A factor graph approach to universal mixture modeling: a general recipe

In this subsection we present the general recipe for computing the posterior distributions over the variables s and model selection variable m in universal mixture models. Section 3.3 provides an illustrative example that aids the exposition in this section. The order in which these two sections are read are a matter of personal preference.

In many practical applications distinct models $p(y_k, s_k | m_k = 1)$ partly overlap in both structure and variables. These models may for example just differ in terms of priors or likelihood functions. Let $f_o(y_o, s_o)$ be the product of factors

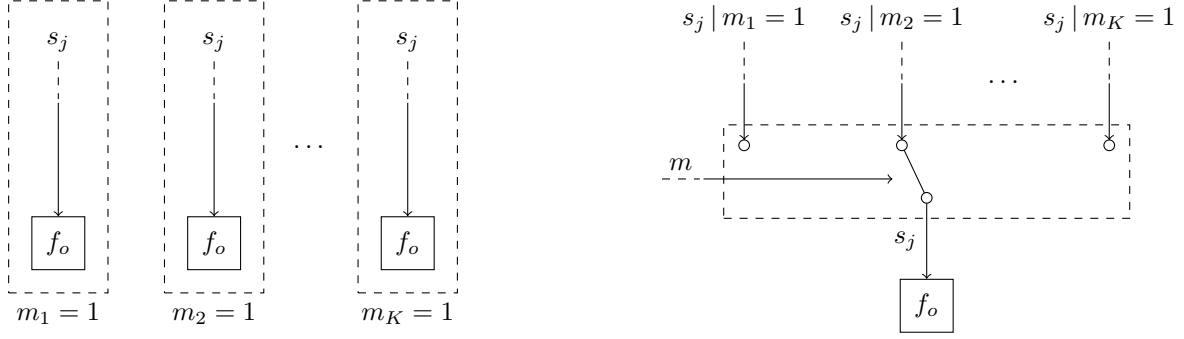


Figure 3: (left) Overview of the traditional process of model comparison. Here inference is performed in a set of K models after which the models are compared. These models may partially overlap in both variables as in structure. Specifically, in this example the variables s_j connect the overlapping factors f_o to the non-overlapping factors. The notation $s_j | m_k = 1$ denotes the variable s_j in the k^{th} model. (right) Our approach to model comparison based on mixture modeling. The different models are combined into a single graph representing a mixture model, where the model selection variable m specifies the component assignment. The variable s_j without conditioning implies that it has been marginalized over the different models m .

which are present in all different factorizable models $p(y_k, s_k | m_k = 1)$, with overlapping variables $s_o = \bigcap_{k=1}^K s_k$ and $y_o = \bigcap_{k=1}^K y_k$. Based on this description we define a universal mixture model as in [2] encompassing all individual models as

$$\begin{aligned}
 p(y, s, m) &= p(m) \prod_{k=1}^K p(y_k, s_k | m_k = 1)^{m_k} \\
 &= p(m) f_o(y_o, s_o) \prod_{k=1}^K \left(\frac{p(y_k, s_k | m_k = 1)}{f_o(y_o, s_o)} \right)^{m_k}, \quad (15)
 \end{aligned}$$

with model selection variable m . Here the overlapping factors are factored out from the mixture components. Figure 3 shows a visualization of the transformation from K distinct models into a single mixture model. With the transformation from the different models into a single mixture model presented in Figure 3, it becomes possible to include the model selection variable m into the same probabilistic model.

In these universal mixture models we are often interested in computing the posterior distributions of 1) the overlapping variables s_o marginalized over the distinct models and of 2) the model selection variable m . Given the posterior distributions $q(s_o | m_k = 1)$ over variables s_o in a single model m_k , we can compute the joint posterior distribution over all overlapping variables $q(s_o)$ as

$$q(s_o) = \mathbb{E}_{q(m)} \left[\prod_{k=1}^K q(s_o | m_k = 1)^{m_k} \right], \quad (16)$$

marginalized over the different models m . In the generic case, this computation follows a three-step procedure. First, the posterior distributions $q(s_k | m_k = 1)$ are computed in the individual submodels through an inference algorithm of choice. Then based on the computed VFE $F_k[q]$ of the individual models, the variational posterior $q(m)$ can be calculated. Finally, the joint posterior distribution $q(s_o)$ can be computed using (16).

Here, we will restrict ourselves to acyclic submodels. We will show that the previously described inference procedure for computing the joint posterior distributions can be performed jointly with the process of model comparison through message passing with scale factors. In order to arrive at this point, we combine the different models into a single mixture model inspired by [2, 3]. Our specification of the mixture model, however, is more general compared to [2, 3] as it does not constrain the hierarchical depth of the overlapping or distinct models and also works for nested mixture models.

Table 1 introduces the novel mixture node, which acts as a switching mechanism between different models, based on the selection variable m . It connects the model selection variables m and the overlapping variables $s_j | m_k = 1$ for the different models m_k , to the variable s_j marginalized over m . Here the variables s_j connect the overlapping to the non-overlapping factors.

The messages in Table 1 are derived in Appendices B.2 and B.3 and can be intuitively understood as follows. The message $\tilde{\mu}_m(m)$ represents the unnormalized distribution over the model evidences corresponding to the individual

Table 1: Table containing (top) the Forney-style factor graph representation of the mixture node. (bottom) The derived outgoing messages for the mixture node. It can be noted that the backward message towards m resembles a scaled categorical distribution and that the forward message towards s_j represents a mixture distribution. Derivations of the messages $\vec{\mu}_m(m)$ and $\vec{\mu}_{s_j}(s_j)$ are presented in Appendices B.2 and B.3, respectively.

Factor node	
Messages	Functional form
$\vec{\mu}_m(m)$	$\prod_{k=1}^K \left(\int \vec{\mu}_{s_j m_k=1}(s_j) \vec{\mu}_{s_j}(s_j) ds_j \right)^{m_k}$
$\vec{\mu}_{s_j}(s_j)$	$\sum_{k=1}^K \vec{\mu}_m(m_k = 1) \vec{\mu}_{s_j m_k=1}(s_j)$
$\vec{\mu}_{s_j m_k=1}(s_j)$	$\vec{\mu}_{s_j}(s_j)$

models. Based on the scale factors of the incoming messages, the model evidences can be computed. The message $\vec{\mu}_{s_j|m_k=1}(s_j)$ equals the incoming message from the likelihood $\vec{\mu}_{s_j}(s_j)$. It will update $s_j | m_k = 1$ as if the k^{th} model is active. The message $\vec{\mu}_{s_j}(s_j)$ represents a mixture distribution over the incoming messages $\vec{\mu}_{s_j|m_k=1}(s_j)$, where the weightings are determined by the message $\vec{\mu}_m(m)$ and the scale factors of the messages $\vec{\mu}_{s_j|m_k=1}(s_j)$. This message can be propagated as a regular message over overlapping model segment yielding the marginal posterior distributions over all variables in the overlapping model segment.

Theorem 3.1. Consider multiple acyclic FFGs. Given the message $\vec{\mu}_{s_j}(s_j)$ in Table 1 that has been marginalized over the different models m . Propagating this message through the factor $f_a(y_a, s_a)$ which overlaps for all models with $s_j \in s_a$, yields again messages which are marginalized over the different models.

Proof. See Appendix A.2. □

3.3 A factor graph approach to universal mixture modeling: an illustrative example

Consider the two probabilistic models

$$p(y, s | m_1 = 1) = p(y | s) p(s | m_1 = 1), \quad (17)$$

$$p(y, s | m_2 = 1) = p(y | s) p(s | m_2 = 1), \quad (18)$$

which share the same likelihood model with a single observed and latent variable y and s , respectively. The model selection variable m is subject to the prior

$$p(m) = \text{Ber}(m | \pi) = \pi^{m_1} (1 - \pi)^{m_2}, \quad (19)$$

with π denoting the success probability. This allows for the specification of the mixture model

$$p(y, s, m) = p(m) p(y | s) \prod_{k=1}^2 p(s | m_k = 1)^{m_k}, \quad (20)$$

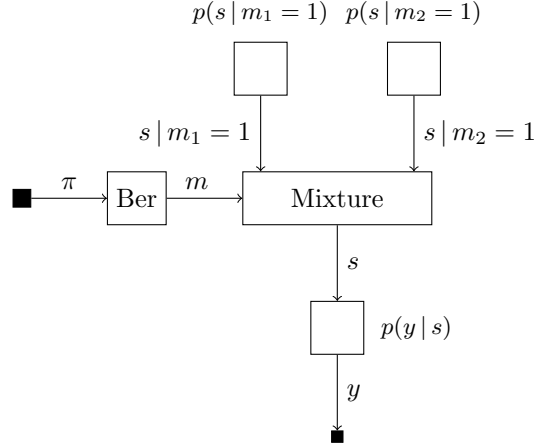


Figure 4: Factor graph visualization of (20) in the example sketched in Section 3.3.

which we visualize in Figure 4.

Suppose we are interested in computing the posterior probabilities $p(s | y = \hat{y})$, marginalized over the distinct models, and $p(m | y = \hat{y})$. The model evidences of both models can be computed using scale factors locally on the edge corresponding to s as

$$p(y = \hat{y} | m_1 = 1) = \int \tilde{\mu}_{s|m_1=1}(s) \tilde{\mu}_s(s) ds = \int p(s | m_1 = 1) p(y = \hat{y} | s) ds,$$

$$p(y = \hat{y} | m_2 = 1) = \int \tilde{\mu}_{s|m_2=1}(s) \tilde{\mu}_s(s) ds = \int p(s | m_2 = 1) p(y = \hat{y} | s) ds,$$

which takes place inside the mixture node for computing $\tilde{\mu}_m(m)$. Together with the forward message over edge m , we obtain the posterior

$$p(m | y = \hat{y}) = \frac{\tilde{\mu}_m(m) \tilde{\mu}_m(m)}{\sum_{k=1}^2 \tilde{\mu}_m(m_k = 1) \tilde{\mu}_m(m_k = 1)} = \frac{p(m) p(y = \hat{y} | m)}{p(y = \hat{y})}. \quad (21)$$

The posterior distribution over s for the first model can be computed as

$$p(s | y = \hat{y}, m_1 = 1) = \frac{\tilde{\mu}_{s|m_1=1}(s) \tilde{\mu}_s(s)}{p(y = \hat{y} | m_1 = 1)}.$$

From (16) we can then compute the posterior distribution over s marginalized over both models as

$$\begin{aligned} p(s | y = \hat{y}) &= p(m_1 = 1 | y = \hat{y}) p(s | y = \hat{y}, m_1 = 1) \\ &\quad + p(m_2 = 1 | y = \hat{y}) p(s | y = \hat{y}, m_2 = 1), \\ &= \frac{p(m_1 = 1) p(y = \hat{y} | m_1 = 1)}{p(y = \hat{y})} \frac{\tilde{\mu}_{s|m_1=1}(s) \tilde{\mu}_s(s)}{p(y = \hat{y} | m_1 = 1)} \\ &\quad + \frac{p(m_2 = 1) p(y = \hat{y} | m_2 = 1)}{p(y = \hat{y})} \frac{\tilde{\mu}_{s|m_2=1}(s) \tilde{\mu}_s(s)}{p(y = \hat{y} | m_2 = 1)}, \\ &= \frac{(p(m_1 = 1) \tilde{\mu}_{s|m_1=1}(s) + p(m_2 = 1) \tilde{\mu}_{s|m_2=1}(s)) \tilde{\mu}_s(s)}{p(y = \hat{y})}. \end{aligned}$$

4 Model comparison methods

In this section, we introduce three Bayesian model comparison methods: model averaging, selection and combination. For each of these methods we describe how to automate them using message passing with the mixture node in Table 1. The factor graph approach here aids the intuitive understanding of the different approaches as their distinctions are sometimes obscure in the literature. As we will show, each method describes an inference procedure on a slightly different model for the model selection variable m , possibly with different variational constraints, as visualized in Figure 5.

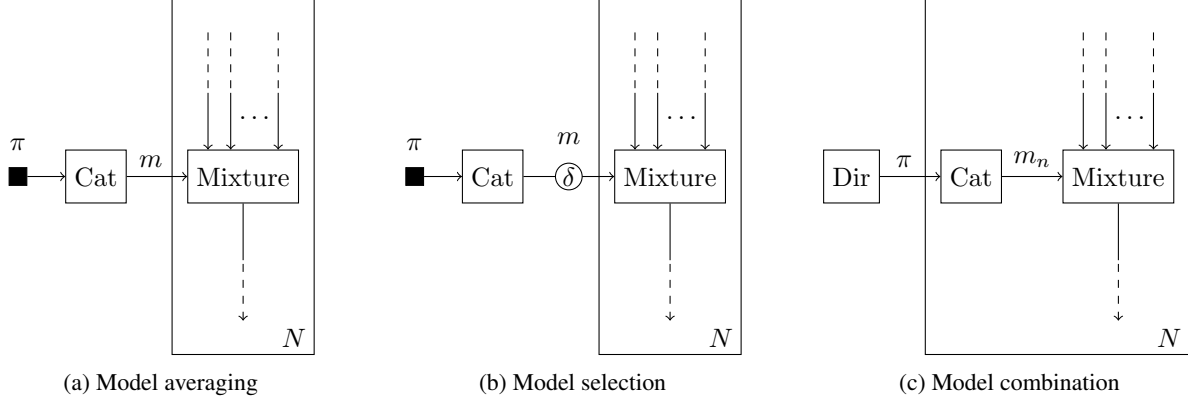


Figure 5: Schematic overview of (a) Bayesian model averaging, (b) selection and (c) combination as specified in Sections 4.1-4.3. This overview explicitly visualizes the structural differences between the prior distributions and form constraints imposed on the model selection variable m . The edges crossing the plates are implicitly connected through equality nodes.

4.1 Bayesian model averaging

Bayesian model averaging (BMA) can be considered the simplest form of model comparison. Yet, despite its simplicity it is often subject to misinterpretation [22]. BMA specifies a categorical prior distribution over the models m as

$$p(m) = \text{Cat}(m | \pi), \quad (22)$$

where π denotes the vector of event probabilities. Contrary to what its naming might imply, BMA does not find the best possible weighted set of models that explains the data [22]. Given a set of possible models, or hypotheses, with BMA the posterior distribution $q(m)$ converges to a Kronecker delta function that selects the single model which is the most likely given the observed set of data [2, 22]. Figure 5a provides a visual representation of Bayesian model averaging.

4.2 Bayesian model selection

Bayesian model selection (BMS) is a further specification of BMA as illustrated in Figure 5b, which selects the model out of a group of models that is the maximum a posteriori (MAP) estimate of m . In addition to the model prior of (22), we add a form constraint [13] to the variable m . Specifically, we constrain the posterior distribution $q(m)$ to be a Kronecker delta function $\delta(\cdot)$, centered around the MAP estimate of m as

$$q(m) = \delta(m - e_k), \quad \text{s.t. } k = \arg \max_k \tilde{\mu}_m(m_k = 1) \tilde{\mu}_m(m_k = 1), \quad (23)$$

where e_k represent the k^{th} Euclidean standard basis vector. Figure 5b visualizes this constraint by the encircled δ on the edge corresponding to the variable m . This form constraint will effectively interrupt the flow of the messages μ_m and instead propagate the computed marginal distribution $q(m)$ back to the connected nodes [13, Theorem 3]. As a result $q(m)$ will be substituted for $\tilde{\mu}_m(m)$ in the message $\tilde{\mu}_{s_j}(s_j)$ in Table 1, which performs a selection on the incoming messages for the outgoing message as $\tilde{\mu}_{s_j}(s_j) = \tilde{\mu}_{s_j|m_k=1}(s_j)$.

4.3 Bayesian model combination

Bayesian model combination (BMC) [1] attempts to solve the problems originating from BMA. BMA converges to the single best model of the group of possible models [2]. In the case that the true model is inside the subsets of models to evaluate, this will correctly identify the true model. However, often the true underlying model is not within this subset and therefore a suboptimal model is selected. In this case, there might actually exist a specific weighted combination of models that outperforms the single best model [22]. BMC is designed in order to find this combination through probabilistic inference. The founding work of [1] presents two approaches for BMC: 1) by performing an extensive search over a discretized subspace of model weightings, and 2) by sampling from a Dirichlet distribution that extends the regular categorical model prior. Here we will illustrate the latter approach using a Dirichlet prior on π , because inference in this model can be executed efficiently using message passing.

Contrary to the previous subsection, every (set of) observation(s) is now modeled by a distinct model m_n , where n indexes the observation. Each variable m_n comprises a 1-of- K binary vector with elements $m_{nk} \in \{0, 1\}$ constrained

by $\sum_{k=1}^K m_{nk} = 1$. We specify the prior distribution

$$p(m_n | \pi) = \text{Cat}(m_n | \pi), \quad (24)$$

where the event probabilities π now appear as a random variable, which is modeled by

$$p(\pi) = \text{Dir}(\pi | \alpha), \quad (25)$$

where α are the concentration parameters. Intuitively, the variable π is shared among all observations, whereas m_n is specific to a single observation, as shown in Figure 5c.

4.3.1 Probabilistic inference for Bayesian model combination

Exact inference in this model is intractable because the posterior over π resembles a mixture of Dirichlet distributions with a number of components that scales exponentially with the number of observations. As a result, previous works in the literature have presented approximate algorithms for performing probabilistic inference in this model, such as sampling [1]. Here we will present two alternative approaches for performing approximate inference in this model.

The first approach concerns constraining the posterior distributions over m_n to be Kronecker delta functions $\delta(\cdot)$ similarly as in Section 4.2 as

$$q(m_n) = \delta(m_n - e_k), \quad \text{s.t. } k = \arg \max_k \vec{\mu}_{m_n}(m_{nk} = 1) \tilde{\mu}_{m_n}(m_{nk} = 1). \quad (26)$$

Here we have chosen the approximate posterior $q(m_n)$ to be centered around the MAP estimate of m_n , however, alternative centers can also be chosen, for example by sampling from $\vec{\mu}_{m_n}(m_{nk} = 1) \tilde{\mu}_{m_n}(m_{nk} = 1)$. Using this constraint the backward message $\tilde{\mu}_\pi(\pi)$ towards π can be computed analytically [23, Appendix A.5]. Batch or offline processing can be performed by an iterative message passing procedure, similarly as in variational message passing [5–7], which requires initialization of the messages $\vec{\mu}_{m_n}(m_n)$ or the marginals $q(m_n)$ in order to break circular dependencies between messages and marginals in the model. However, this approach also lends itself towards an online setting with streaming observations, although the results are heavily influenced by the prior $p(\pi)$. In Section 5.1 we describe an approach to cope with this initialization problem.

An alternative approach for performing approximate inference in an offline manner is obtained by variational message passing [5–7]. The true posterior distribution $p(\pi, m_1, \dots, m_N | D)$ is in this case approximated by the variational posterior distribution $q(\pi, m_1, \dots, m_N)$ being subject to a naive mean-field factorization as

$$p(\pi, m_1, \dots, m_N | D) \approx q(\pi, m_1, \dots, m_N) = q(\pi) \prod_{n=1}^N q(m_n), \quad (27)$$

where the individual variational distributions are constrained to have the functional forms

$$q(\pi) = \text{Dir}(\pi | \tilde{\alpha}), \quad (28a)$$

$$q(m_n) = \text{Cat}(m_n | \tilde{\pi}_n), \quad (28b)$$

where the $\tilde{\cdot}$ accent is used to indicate the parameters of the variational posterior distributions. Variational message passing minimizes the variational free energy by iterating the computation of variational messages and posteriors until convergence. The corresponding variational message passing update rules are derived in [23, Appendix A.5].

5 Experiments

In this section a set of experiments are presented for the previously presented message passing-based model comparison techniques. Section 5.1 verifies the basic operations of the inference procedures for model averaging, selection and combination for data generated from a known mixture distribution. In Section 5.2 the model comparison approaches are validated on application-based examples.

All experiments have been performed using the scientific programming language Julia [24] with the state-of-the-art probabilistic programming package RxInfer.jl [25]. The mixture node specified in Section 3.2 has been integrated in its message passing engine ReactiveMP.jl [26, 27]. Aside from the results presented in the upcoming subsections, interactive Pluto.jl notebooks are made available online², allowing the reader to change hyperparameters in real-time.

²All experiments are publicly available at <https://github.com/biaslab/AutomatingModelComparison>.

5.1 Verification experiments

For verification of the mixture node in Table 1, $N = \{1, 5, 10, 100, 1000\}$ observations y_n have been generated from the mixture distribution

$$p(y_n) = 0.2\mathcal{N}(y_n | -4, 1 + \sigma^2) + 0.5\mathcal{N}(y_n | 0, 1 + \sigma^2) + 0.3\mathcal{N}(y_n | 5, 1 + \sigma^2), \quad (29)$$

where $\mathcal{N}(y_n | \mu, \sigma^2)$ represents a normal distribution with mean μ and variance σ^2 . σ^2 represents the additional observation noise variance. For the obtained data we construct the probabilistic model

$$p(x_n | m) = \mathcal{N}(x_n | -4, 1)^{m_1} \mathcal{N}(x_n | 0, 1)^{m_2} \mathcal{N}(x_n | 5, 1)^{m_3}, \quad (30a)$$

$$p(y_n | x_n) = \mathcal{N}(y_n | x_n, \sigma^2), \quad (30b)$$

which gets completed by the structures imposed on m as introduced in Section 4. Depending on the comparison method as outlined in Sections 4.1-4.3 we added an uninformative categorical prior on z or an uninformative Dirichlet prior on the event probabilities π that model z . The aim is to infer the marginal (approximate) posterior distributions over component assignment variable z , for model averaging and selection, and over event probabilities π , for model combination.

For online Bayesian model combination preliminary experiments showed that the results relied significantly on the initial prior $p(\pi)$. Choosing this term to be uninformative, i.e. $\alpha_k \ll 1 \forall k$ and $\alpha_i = \alpha_j \forall i, j$, lead to a posterior distribution which became dominated by the inferred cluster assignment of the first observation. As a result, the predictive class probability approached a delta distribution, centered around the class label of the first observation, leading to all consecutive observations being assigned to the same cluster. To remedy this undesirable behaviour, the prior $p(\pi)$ was chosen to prefer uniformly distributed class labels, i.e. $\alpha_k \gg 1 \forall k$ and $\alpha_i = \alpha_j \forall i, j$. After the inference procedure was completed the informativeness of this prior was removed using Bayesian model reduction [18, 19], where the approximate posterior over π was recomputed based on an alternative uninformative prior.

Figure 6 shows the inferred posterior distributions of z or the predictive distributions for z obtained from the posterior distributions $q(\pi)$, for an observation noise variance $\sigma^2 = 0.1$. From the results, it can be observed that Bayesian model averaging rapidly converges to a single cluster with high probability, similar to Bayesian model selection. The selected cluster corresponds to the cluster with the highest mixing weight in (29). Contrary to Bayesian model selection, the alternative event probabilities obtained with Bayesian model averaging are non-zero. Both Bayesian model combination approaches do not converge to a single cluster assignment as expected. Instead, they better recover the mixing weights in the data-generating distribution. The discrepancies here are caused by the overlapping support of the different components.

5.2 Validation experiments

Aside from verifying the correctness of the message passing implementations of Section 4 using the mixture node, this section further illustrates its usefulness in a set of validation experiments, covering real-world problems.

5.2.1 Mixed models

In order to illustrate an application of the mixture node from Table 1, we show how it can be used in a mixed model where it connects continuous to discrete variables. Consider the hypothetical situation where we wish to fit a mixture with fixed components but unknown mixing coefficients to some set of observations. To highlight the generality of the mixture node, the mixture components are chosen to reflect shifted product distributions, where the possible shifts are limited to a discrete set of values. The assumed probabilistic model of a single observation y is given by

$$p(a) = \mathcal{N}(a | 0.5, 1), \quad (31a)$$

$$p(b) = \mathcal{N}(b | 0, 1), \quad (31b)$$

$$p(c | z) = \delta(c + 0.2)^{z_1} \delta(c + 1.8)^{z_2} \delta(c - 0.9)^{z_3}, \quad (31c)$$

$$p(z) = \text{Cat}(z | \mathbf{1}_3/3), \quad (31d)$$

$$p(y | a, b, c) = \delta(y - (ab + c)). \quad (31e)$$

The variables a, b are latent variables defining the product distribution. c specifies the shift introduced on this distribution, which is picked by the selector variable z , comprising a 1-of-3 binary vector with elements $z_k \in \{0, 1\}$ constrained by $\sum_{k=1}^3 z_k = 1$. $\mathbf{1}_K$ denotes a vector of ones of length K . The goal is to infer the posterior distribution of z and to therefore fit this exotic mixture model to some set of data.

We perform offline probabilistic inference in this model using Bayesian model averaging and Bayesian model combination. For the latter approach we extend the prior on z with a Dirichlet distribution following Section 4.3 and by

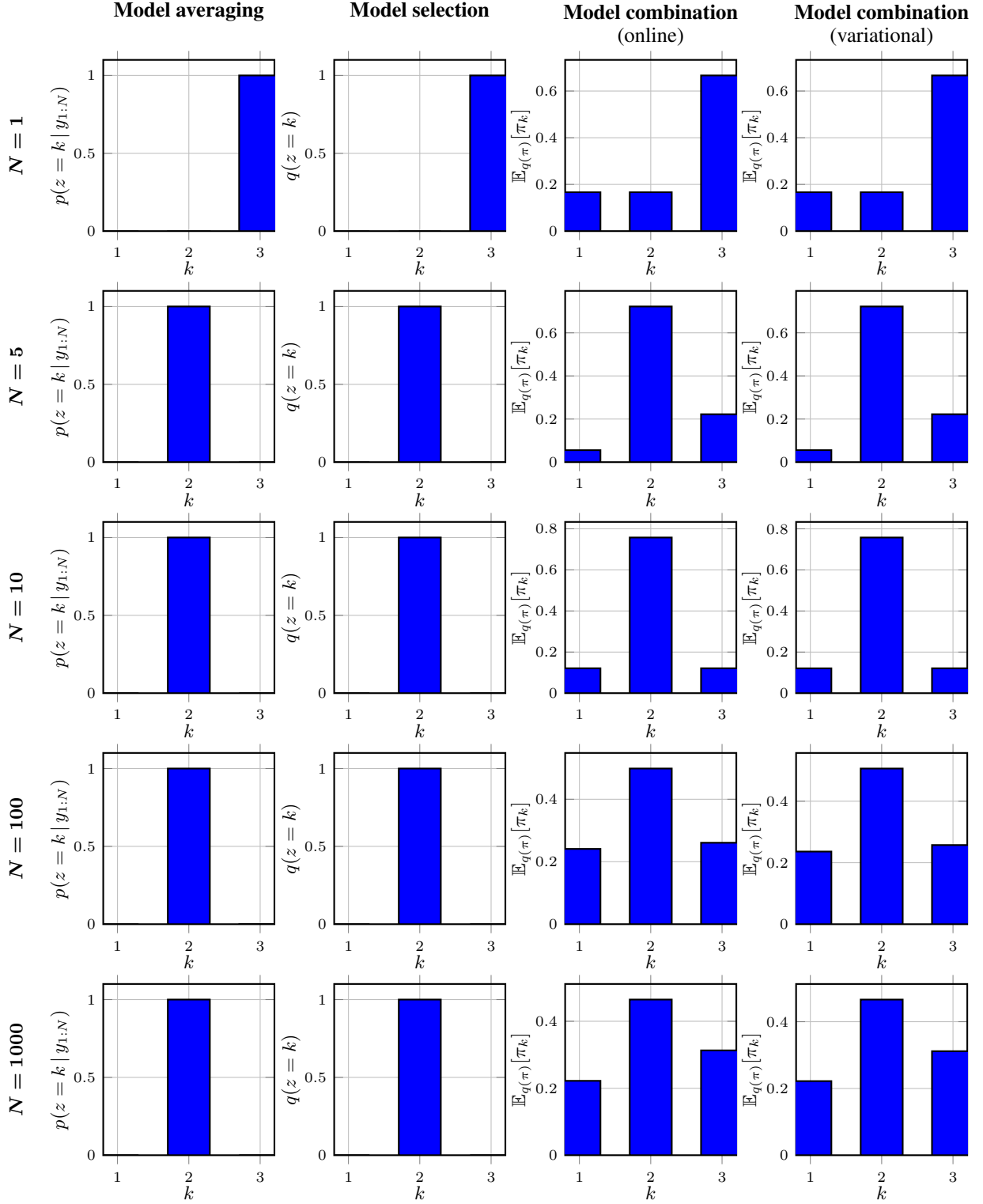


Figure 6: Visualization of the verification experiments as specified in Section 5.1. The individual plots show the (predictive) posterior distributions for the assignment variable in (29) for $N = \{1, 5, 10, 100, 1000\}$ observations as computed using the different methods outlined in Sections 4.1-4.3.

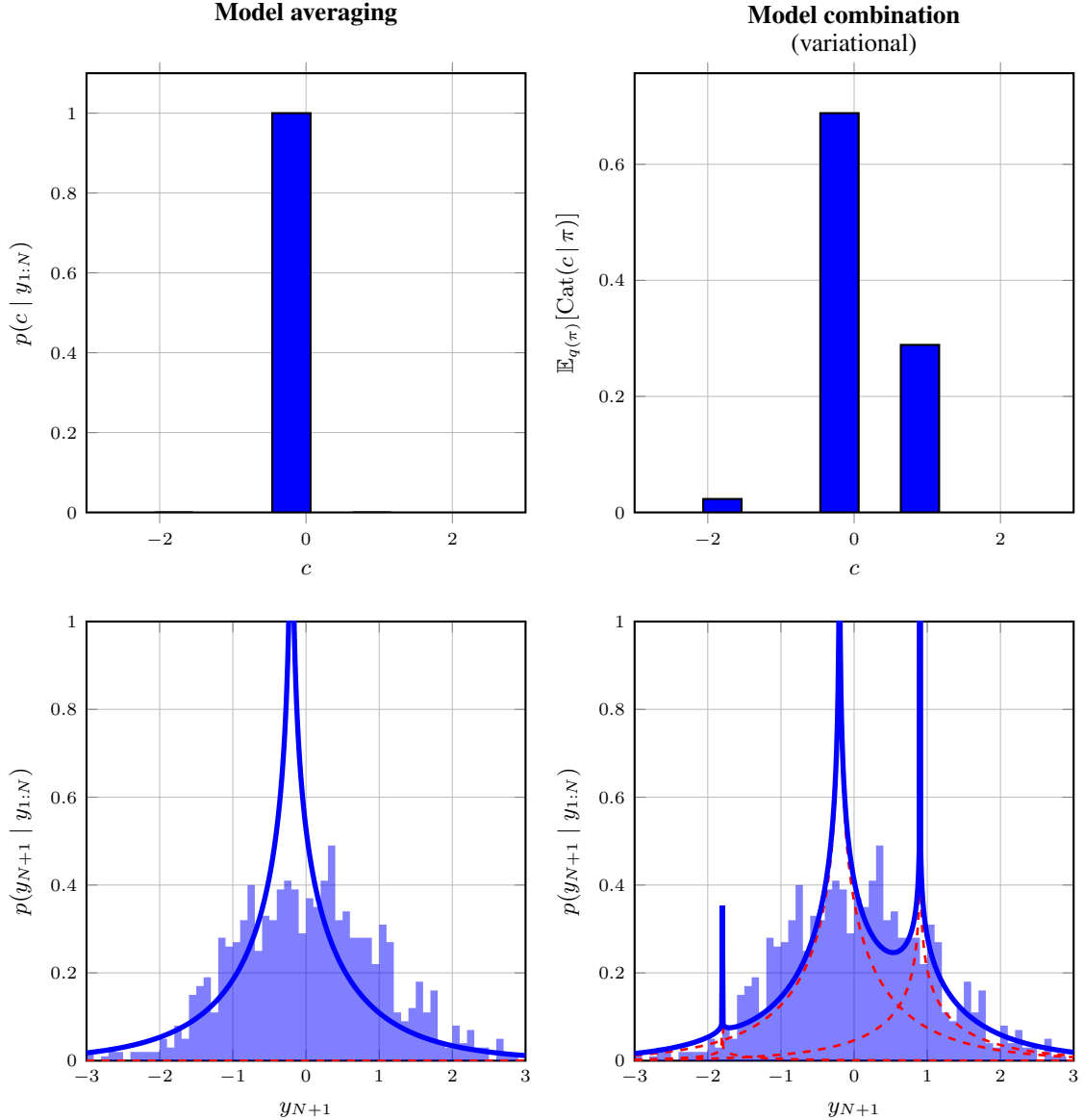


Figure 7: Inference results of the mixed model as described in Section 5.2.1. The inference procedure is performed by (left) Bayesian model averaging and (right) Bayesian model combination under a variational mean-field factorization. (top) The posterior estimate for the shift c . (bottom) The predictive posterior distribution for new observations in blue with underlying components in red.

assuming a variational mean-field factorization. The shifted product distributions do not yield tractable closed-form messages, therefore these distributions are approximated following [28]. Figure 7 shows the obtained data fit on a data set of 1500 observations drawn from a standard normal distribution. This distribution does not reflect the used model in (31) on purpose to illustrate its behaviour when the true underlying model is not one of the components. As expected model averaging converges to the most dominant component, whereas model combination attempts to improve the fit by combining the different components with fixed shifts.

5.2.2 Voice activity detection

In this section we illustrate a message passing approach to voice activity detection in speech that is corrupted by additive white Gaussian noise using the mixture node from Table 1. We model speech signal s_t as a first-order auto-regressive

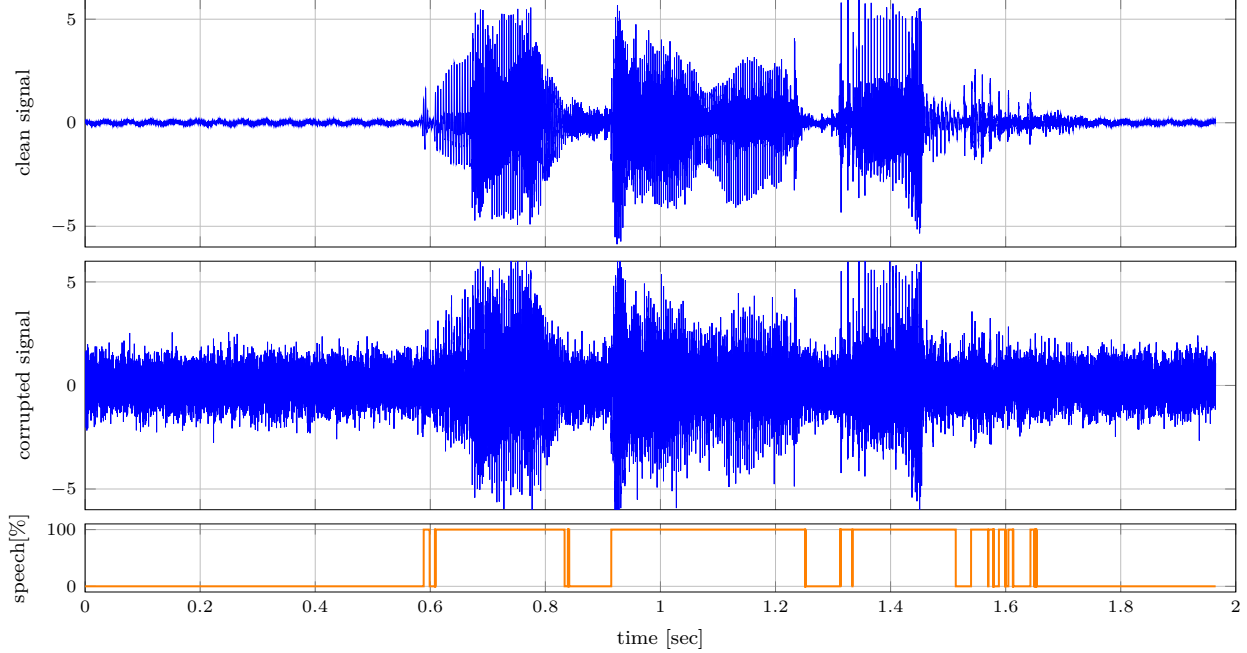


Figure 8: Results of the voice activity detection experiment as specified in Section 5.2.2. The figure shows (top) the clean signal, (middle) the clean signal corrupted by additive white Gaussian noise and (bottom) the inferred speech probability.

process as

$$p(s_t | s_{t-1}) = \mathcal{N}(s_t | \rho s_{t-1}, \sigma^2), \quad (32)$$

with auto-regressive parameter ρ and process noise variance σ^2 . The absence of speech is modeled by independent and identically distributed variables n_t , which are enforced to be close to 0 as

$$p(n_t) = \mathcal{N}(n_t | 0, 0.01). \quad (33)$$

We model our observations by the mixture distribution, where we include the corruption from the additive white Gaussian noise, as

$$p(y_t | s_t, n_t, z_t) = \mathcal{N}(y_t | s_t, 0.5)^{z_{t1}} \mathcal{N}(y_t | n_t, 0.5)^{z_{t2}}. \quad (34)$$

Here z_t indicates the voice activity of the observed signal as a 1-of-2 binary vector with elements $z_{tk} \in \{0, 1\}$ constrained by $\sum_{k=1}^2 z_{tk} = 1$. Because periods of speech are often preceded by more speech, we add temporal dynamics to z_t as

$$p(z_t | z_{t-1}) = \text{Cat}(z_t | \mathbf{T}z_{t-1}), \quad (35)$$

where the transition matrix is specified as $\mathbf{T} = [0.99999, 10^{-5}; 10^{-5}, 0.99999]$.

Figure 8 shows the clean and corrupted audio signals. The audio is sampled with a sampling frequency of 16 kHz. The corrupted signal is used for inferring z_t which is presented in the bottom plot. Despite the corruption inflicted on the audio signal, this presented simple model is capable of detecting voice effectively as illustrated in the bottom plot of Figure 8.

6 Discussion

The unifying view between probabilistic inference and model comparison as presented by this paper allows us to leverage the efficient message passing schemes for both tasks. Interestingly, this view allows for the use of belief propagation [29], variational message passing [5–7] and other message passing-based algorithms around the subgraph connected to the model selection variable m . This insight gives rise to a novel class of model comparison algorithms, where the prior on the model selection variable is no longer constrained to be a categorical distribution, but where we now can straightforwardly introduce hierarchical and/or temporal dynamics. Furthermore, a consequence of the automatability of the message passing algorithms is that these model comparison algorithms can easily and efficiently be implemented, without the need of error-prone and time-consuming manual derivations.

The presented approach is especially convenient when the model allows for the use of scale factors [15, Ch.6], [16]. In this way we can efficiently compute the model evidence as shown in [16]. The introduced mixture node in Table 1 consecutively enables a simple model specification as illustrated in the source code of our experiments.

A limitation of the scale factors is that they can only be efficiently computed when the model submits to exact inference [16]. Extensions of the scale factors towards a variational setting would allow the use of the mixture node with a bigger variety of models. If this limitation is resolved, then the introduced approach can be combined with more complicated models, such as for example Bayesian neural networks, whose performance is measured by the variational free energy, see e.g. [30, 31]. This provides a novel solution to multi-task machine learning problems where the number of tasks is not known beforehand [32]. Each Bayesian neural network can then be trained for a specific task and additional components or networks can be added if appropriate.

7 Conclusions

This paper bridges the gap between probabilistic inference for states and parameters, and for model comparison, allowing for the simultaneous automation of both tasks. It is shown that model comparison can be performed by message passing on a graph terminated by a node that captures the performances of the different submodels, as motivated from a variational free energy perspective. In the case where the model submits to exact inference, we can efficiently implement model comparison using our newly proposed mixture node, which leverages the efficiently computed scale factors. Based on this node description, we differentiate between model averaging, selection, and combination through the (hierarchical) prior and posterior constraints on the selection variable.

Acknowledgments

This work was partly financed by GN Hearing A/S. The authors would like to thank the BIASlab team members for various insightful discussions related to this work.

References

- [1] K. Monteith, J. L. Carroll, K. Seppi, and T. Martinez, “Turning Bayesian model averaging into Bayesian model combination,” in *The 2011 International Joint Conference on Neural Networks*, San Jose, CA, USA, Jul. 2011, pp. 2657–2663, iSSN: 2161-4407.
- [2] K. Kamary, K. Mengersen, C. P. Robert, and J. Rousseau, “Testing hypotheses via a mixture estimation model,” Dec. 2018, arXiv:1412.2044 [stat]. [Online]. Available: <http://arxiv.org/abs/1412.2044>
- [3] M. Keller and K. Kamary, “Bayesian model averaging via mixture model estimation,” Aug. 2018, arXiv:1711.10016 [stat]. [Online]. Available: <http://arxiv.org/abs/1711.10016>
- [4] T. Minka and J. Winn, “Gates,” in *Advances in Neural Information Processing Systems 21*. Curran Associates, Inc., 2009, pp. 1073–1080. [Online]. Available: <http://papers.nips.cc/paper/3379-gates.pdf>
- [5] J. M. Winn, “Variational Message Passing and its Applications,” Ph.D. dissertation, University of Cambridge, Cambridge, United Kingdom, 2004.
- [6] J. Winn and C. M. Bishop, “Variational Message Passing,” *Journal of Machine Learning Research*, pp. 661–694, 2005.
- [7] J. Dauwels, “On Variational Message Passing on Factor Graphs,” in *2007 IEEE International Symposium on Information Theory*, Nice, France, Jun. 2007, pp. 2546–2550, iSSN: 2157-8117.
- [8] T. P. Minka, “Expectation Propagation for Approximate Bayesian Inference,” in *Proceedings of the Seventeenth Conference on Uncertainty in Artificial Intelligence*. San Francisco, CA, USA: Morgan Kaufmann Publishers Inc., 2001, pp. 362–369. [Online]. Available: <http://dl.acm.org/citation.cfm?id=2074022.2074067>
- [9] G. Forney, “Codes on graphs: normal realizations,” *IEEE Transactions on Information Theory*, vol. 47, no. 2, pp. 520–548, Feb. 2001.
- [10] H.-A. Loeliger, “An introduction to factor graphs,” *IEEE Signal Processing Magazine*, vol. 21, no. 1, pp. 28–41, Jan. 2004.
- [11] H.-A. Loeliger, J. Dauwels, J. Hu, S. Korl, L. Ping, and F. R. Kschischang, “The Factor Graph Approach to Model-Based Signal Processing,” *Proceedings of the IEEE*, vol. 95, no. 6, pp. 1295–1322, Jun. 2007. [Online]. Available: <http://ieeexplore.ieee.org/document/4282128/>

- [12] F. Kschischang, B. Frey, and H.-A. Loeliger, "Factor graphs and the sum-product algorithm," *IEEE Transactions on Information Theory*, vol. 47, no. 2, pp. 498–519, Feb. 2001.
- [13] I. Şenöz, T. van de Laar, D. Bagaev, and B. de Vries, "Variational Message Passing and Local Constraint Manipulation in Factor Graphs," *Entropy*, vol. 23, no. 7, p. 807, Jul. 2021. [Online]. Available: <https://www.mdpi.com/1099-4300/23/7/807>
- [14] J. Dauwels, S. Korl, and H.-A. Loeliger, "Expectation maximization as message passing," in *Proceedings. International Symposium on Information Theory, 2005. ISIT 2005.* Adelaide, Australia: IEEE, 2005, pp. 583–586. [Online]. Available: <http://ieeexplore.ieee.org/document/1523402/>
- [15] C. Reller, "State-space methods in statistical signal processing: New ideas and applications," Ph.D. dissertation, ETH Zurich, 2013. [Online]. Available: <http://hdl.handle.net/20.500.11850/65488>
- [16] H. M. Nguyen, B. van Erp, İ. Şenöz, and B. de Vries, "Efficient Model Evidence Computation in Tree-structured Factor Graphs," in *2022 IEEE Workshop on Signal Processing Systems (SiPS)*, Nov. 2022, pp. 1–6, iSSN: 2374-7390.
- [17] C. M. Bishop, *Pattern recognition and machine learning*, ser. Information science and statistics. New York: Springer, 2006.
- [18] K. Friston and W. Penny, "Post hoc Bayesian model selection," *NeuroImage*, vol. 56, no. 4, pp. 2089–2099, Jun. 2011. [Online]. Available: <http://www.sciencedirect.com/science/article/pii/S1053811911003417>
- [19] K. Friston, T. Parr, and P. Zeidman, "Bayesian model reduction," *arXiv:1805.07092 [stat]*, Oct. 2019, arXiv: 1805.07092. [Online]. Available: <http://arxiv.org/abs/1805.07092>
- [20] T. Parr and K. J. Friston, "Generalised free energy and active inference," *Biological Cybernetics*, vol. 113, no. 5, pp. 495–513, Dec. 2019. [Online]. Available: <https://doi.org/10.1007/s00422-019-00805-w>
- [21] J. S. Yedidia, W. T. Freeman, and Y. Weiss, "Bethe free energy, Kikuchi approximations, and belief propagation algorithms," *Advances in neural information processing systems*, vol. 13, 2001. [Online]. Available: <https://www.merl.com/publications/docs/TR2001-16.pdf>
- [22] T. P. Minka, "Bayesian model averaging is not model combination," *Available electronically at http://www.stat.cmu.edu/minka/papers/bma.html*, 2000. [Online]. Available: <https://tminka.github.io/papers/minka-bma-isnt-mc.pdf>
- [23] T. van de Laar, "Automated design of Bayesian signal processing algorithms," Ph.D. dissertation, Technische Universiteit Eindhoven, Eindhoven, the Netherlands, 2019, oCLC: 8153707591.
- [24] J. Bezanson, A. Edelman, S. Karpinski, and V. B. Shah, "Julia: A Fresh Approach to Numerical Computing," *SIAM Review*, vol. 59, no. 1, pp. 65–98, Jan. 2017, publisher: Society for Industrial and Applied Mathematics. [Online]. Available: <https://epubs.siam.org/doi/10.1137/141000671>
- [25] D. Bagaev, A. Podusenko, and B. De Vries, "RxInfer: A Julia package for reactive real-time Bayesian inference," *Journal of Open Source Software*, vol. 8, no. 84, p. 5161, Apr. 2023. [Online]. Available: <https://joss.theoj.org/papers/10.21105/joss.05161>
- [26] D. Bagaev and B. de Vries, "Reactive Message Passing for Scalable Bayesian Inference," *Scientific Programming*, vol. 2023, p. 6601690, May 2023, publisher: Hindawi. [Online]. Available: <https://doi.org/10.1155/2023/6601690>
- [27] D. Bagaev, B. van Erp, A. Podusenko, and B. de Vries, "ReactiveMP.jl: A Julia package for reactive variational Bayesian inference," *Software Impacts*, vol. 12, p. 100299, May 2022. [Online]. Available: <https://www.sciencedirect.com/science/article/pii/S2665963822000422>
- [28] G. Cui, X. Yu, S. Iommelli, and L. Kong, "Exact Distribution for the Product of Two Correlated Gaussian Random Variables," *IEEE Signal Processing Letters*, vol. 23, no. 11, pp. 1662–1666, Nov. 2016, conference Name: IEEE Signal Processing Letters.
- [29] J. Pearl, "Reverend Bayes on Inference Engines: A Distributed Hierarchical Approach," in *Proceedings of the American Association for Artificial Intelligence National Conference on AI*, Pittsburgh, 1982, pp. 133–136.
- [30] C. Blundell, J. Cornebise, K. Kavukcuoglu, and D. Wierstra, "Weight Uncertainty in Neural Networks," May 2015, arXiv:1505.05424 [cs, stat]. [Online]. Available: <http://arxiv.org/abs/1505.05424>
- [31] M. Haussmann, F. A. Hamprecht, and M. Kandemir, "Sampling-Free Variational Inference of Bayesian Neural Networks by Variance Backpropagation," *arXiv:1805.07654 [cs, stat]*, Jun. 2019, arXiv: 1805.07654. [Online]. Available: <http://arxiv.org/abs/1805.07654>
- [32] S. Ruder, "An Overview of Multi-Task Learning in Deep Neural Networks," Jun. 2017, arXiv:1706.05098 [cs, stat]. [Online]. Available: <http://arxiv.org/abs/1706.05098>

- [33] K. Murphy, Y. Weiss, and M. I. Jordan, “Loopy Belief Propagation for Approximate Inference: An Empirical Study,” in *Proceedings of the Fifteenth Conference on Uncertainty in Artificial Intelligence*, Stockholm, Sweden, 1999, arXiv: 1301.6725. [Online]. Available: <http://arxiv.org/abs/1301.6725>

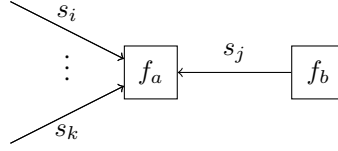


Figure 9: Visualisation of a subgraph.

A Proofs

A.1 Proof of Theorem 2.1

This proof follows a similar recipe as [13, Appendix D.3]. Consider the induced subgraph in Figure 9. The node-local and edge-specific marginals $q_a(s_a)$ and $q_j(s_j)$, respectively, obtained by belief propagation or sum-product message passing as the fixed points of (5) are given by

$$q_a(s_a) = \frac{1}{Z_a} f_a(y = \hat{y}, s_a) \prod_{i \in \mathcal{E}(a)} \bar{\mu}_{s_i}(s_i), \quad (36a)$$

$$q_j(s_j) = \frac{1}{Z_j} \bar{\mu}_{s_j}(s_j) \bar{\mu}_{s_j}(s_j), \quad (36b)$$

as shown in [13, Theorem 1], with node-local and edge-specific normalization constants

$$Z_a = \int f_a(y = \hat{y}, s_a) \prod_{i \in \mathcal{E}(a)} \bar{\mu}_{s_i}(s_i) ds_a, \quad (37a)$$

$$Z_j = \int \bar{\mu}_{s_j}(s_j) \bar{\mu}_{s_j}(s_j) ds_j. \quad (37b)$$

As shown in [13, Appendix D.3] the normalization constants are equal $Z_a = Z_j$. As this holds for all variables $s_j \in s_a$, we can deduce that $Z_i = Z_j \forall i, j \in \mathcal{E}(a)$ also holds. Similarly, this property remains valid for adjacent nodes, allowing us to write

$$Z_a = Z_j \quad \text{s.t. } a \in \mathcal{V}, j \in \mathcal{E}. \quad (38)$$

This property stipulates that the normalization constants of all (joint) marginal distributions are equal if the solutions correspond to the fixed points of (5) under sum-product message passing. As the normalization constant equals the model evidence, we can compute the model evidence on any edge and around any node in our graph. The fixed-point assumption is only violated in the case of cyclic graph where we perform loopy belief propagation [33].

A.2 Proof of Theorem 3.1

The arbitrary outward message $\bar{\mu}_{s_k}(s_k)$ from the node $f_a(y = \hat{y}, s_a)$ can be computed using the sum-product message passing update rule in (5). Substitution of the definition of $\bar{\mu}_{s_j}(s_j)$ of (44) in this update rules yields

$$\begin{aligned} \bar{\mu}_{s_k}(s_k) &= \int \bar{\mu}_{s_j}(s_j) \prod_{\substack{i \neq j \\ i \neq k}} \bar{\mu}_{s_i}(s_i) f_a(y = \hat{Y}, s_a) ds_{a \setminus k}, \\ &= \int \left(\sum_{k=1}^K \bar{\mu}_m(m_k = 1) \bar{\mu}_{s_j | m_k=1}(s_j) \right) \prod_{\substack{i \neq j \\ i \neq k}} \bar{\mu}_{s_i}(s_i) f_a(y = \hat{y}, s_a) ds_{a \setminus k}, \\ &= \sum_{k=1}^K \bar{\mu}_m(m_k = 1) \int \bar{\mu}_{s_j | m_k=1}(s_j) \prod_{\substack{i \neq j \\ i \neq k}} \bar{\mu}_{s_i}(s_i) f_a(y = \hat{y}, s_a) ds_{a \setminus k}, \\ &= \sum_{k=1}^K \bar{\mu}_m(m_k = 1) \bar{\mu}_{s_k | m_k=1}(s_k), \end{aligned} \quad (39)$$

where we identify the same form as compared to $\bar{\mu}_{s_j}(s_j)$.

B Derivations

B.1 Derivation of variational free energy decomposition for mixture models

Following is the derivation of (12):

$$\begin{aligned}
F[q] &= \mathbb{E}_{q(s,m)} \left[\ln \frac{q(s,m)}{p(y = \hat{y}, s, m)} \right] \\
&= \mathbb{E}_{q(s,m)} \left[\ln \frac{q(m) \prod_{k=1}^K q(s_k | m_k = 1)^{m_k}}{p(m) \prod_{k=1}^K p(y_k = \hat{y}_k, s_k | m_k = 1)^{m_k}} \right] \\
&= \mathbb{E}_{q(s,m)} \left[\ln \frac{q(m)}{p(m)} \right] + \mathbb{E}_{q(s,m)} \left[\sum_{k=1}^K m_k \ln \left(\frac{q(s_k | m_k = 1)}{p(y_k = \hat{y}_k, s_k | m_k = 1)} \right) \right] \\
&= \mathbb{E}_{q(s,m)} \left[\ln \frac{q(m)}{p(m)} \right] + \mathbb{E}_{q(s,m)} \left[\prod_{k=1}^K \left(\ln \frac{q(s_k | m_k = 1)}{p(y_k = \hat{y}_k, s_k | m_k = 1)} \right)^{m_k} \right] \\
&= \mathbb{E}_{q(m)} \left[\ln \frac{q(m)}{p(m)} \right] + \mathbb{E}_{q(m)} \left[\prod_{k=1}^K \mathbb{E}_{q(s_k | m_k = 1)} \left[\ln \frac{q(s_k | m_k = 1)}{p(y_k = \hat{y}_k, s_k | m_k = 1)} \right]^{m_k} \right] \\
&= \mathbb{E}_{q(m)} \left[\ln \frac{q(m)}{p(m)} \right] + \mathbb{E}_{q(m)} \left[\prod_{k=1}^K (F_k[q])^{m_k} \right]
\end{aligned}$$

The step from the third to fourth line is the result of the variable m being one-hot coded. As a result only a single m_k equals 1 and all others are constrained to be 0. Therefore we can obtain the identity

$$\prod_{k=1}^K a_k^{m_k} = \sum_{k=1}^K m_k a_k, \quad \text{s.t. } \sum_{k=1}^K m_k = 1 \text{ and } m_k \in \{0, 1\} \forall k$$

which one might recognize as the different representations of the probability mass function of a categorical distribution.

B.2 Derivation of message $\tilde{\mu}_m(m)$

Consider the variable $s_j \in s_o$ in the context of Table 1, where we wish to compute the backwards message $\tilde{\mu}_m(m)$ towards m . As shown in [20] the posterior $q(m)$ can be obtained through functional optimization of (12). Following the approach stipulated in [13], the solution for $q(m)$ follows the form of (6), as

$$q(m) \propto \tilde{\mu}_m(m) \tilde{\mu}_m(m) = \tilde{\mu}_m(m) f(m), \quad (40)$$

where $\tilde{\mu}_m(m)$ denotes the message towards m , not originating from $f(m)$.

Under the assumptions of acyclicity and tractability we obtain

$$\exp(-F_k[q]) = Z_k = \int \tilde{\mu}_{s_j | m_k = 1}(s_j) \tilde{\mu}_{s_j | m_k = 1}(s_j) ds_j \quad (41)$$

holds, from which we obtain the message

$$\tilde{\mu}_m(m) = f(m) = \prod_{k=1}^K \left(\int \tilde{\mu}_{s_j | m_k = 1}(s_j) \tilde{\mu}_{s_j | m_k = 1}(s_j) ds_j \right)^{m_k}, \quad (42)$$

where substitution of (41) into the definition of $f(m)$ in (14) yields the message $\tilde{\mu}_m(m)$ in Table 1. Here we leverage scale factors inside the mixture node to compute the normalization constants of the different models.

B.3 Derivation of message $\vec{\mu}_{s_j}(s_j)$

Consider again the variable $s_j \in s_o$ of which we now wish to compute its posterior distribution $q(s_j)$. Substitution of $q(s_j | m_k = 1)$ in (6) and $\vec{\mu}_m(m)$ in (42) into (16) yields

$$\begin{aligned}
q(s_j) &= \mathbb{E}_{q(m)} \left[\prod_{k=1}^K q(s_j | m_k)^{m_k} \right], \\
&= \sum_{k=1}^K q(m_k) q(s_j | m_k), \\
&= \sum_{k=1}^K \frac{\vec{\mu}_m(m_k = 1) \bar{\mu}_m(m_k = 1)}{\sum_{k=1}^K \vec{\mu}_m(m_k = 1) \bar{\mu}_m(m_k = 1)} \frac{\vec{\mu}_{s_j|m_k}(s_j) \bar{\mu}_{s_j|m_k=1}(s_j)}{\int \vec{\mu}_{s_j|m_k=1}(s_j) \bar{\mu}_{s_j|m_k=1}(s_j) ds_j}, \\
&= \frac{1}{\sum_{k=1}^K \vec{\mu}_m(m_k = 1) \bar{\mu}_m(m_k = 1)} \sum_{k=1}^K \vec{\mu}_m(m_k = 1) \bar{\mu}_m(m_k = 1) \frac{\vec{\mu}_{s_j|m_k=1}(s_j) \bar{\mu}_{s_j|m_k=1}(s_j)}{\bar{\mu}_m(m_k = 1)}, \\
&= \frac{1}{Z_m} \sum_{k=1}^K \vec{\mu}_m(m_k = 1) \bar{\mu}_{s_j|m_k=1}(s_j) \bar{\mu}_{s_j|m_k=1}(s_j),
\end{aligned} \tag{43}$$

where $Z_m = \sum_{k=1}^K \vec{\mu}_m(m_k = 1) \bar{\mu}_m(m_k = 1)$. Furthermore, as a result of the assumption $s_j \in s_o$ being located in the overlapping model section, one of the sum-product messages towards s_j is independent of the model m_k , i.e. either $\bar{\mu}_{s_j|m_k=1}(s_j) = \bar{\mu}_{s_j}(s_j)$ or $\vec{\mu}_{s_j|m_k=1}(s_j) = \vec{\mu}_{s_j}(s_j)$ holds. In the situation sketched in Table 3 we assume the latter. In this case we obtain the identity

$$Z_m q(s_j) = \underbrace{\left(\sum_{k=1}^K \vec{\mu}_m(m_k = 1) \bar{\mu}_{s_j|m_k=1}(s_j) \right)}_{\bar{\mu}_{s_j}(s_j)} \bar{\mu}_{s_j}(s_j), \tag{44}$$

from which the message $\bar{\mu}_{s_j}(s_j)$ in Table 1 can be identified.